Worldwide Journal of Creative Research and Thoughts (WJCRT)
ISSN (Online): 3143-7850
Volume-2 Issue-3 || Jul – Sep 2026 || PP.25– 32
https://wjcrt.org/

The Role of Computer Vision in Automating Microscopic Data Interpretation

Sumit Malhotra
Assistant Professor
Chandigarh University
Gharuan, Mohali,Punjab ,140413
Orcid id- https://orcid.org/0009-0000-6232-1510

http://www.wjcrt.org/ || Vol. 2 No. 3 (2026): September Issue

Date of Submission: 04-08-2026 **Date of Acceptance:** 18-08-2026 **Date of Publication:** 04-09-2026

Abstract— Microscopic imaging is central to biological research, pathology, microbiology, and cellular diagnostics, yet interpretation of microscopy data continues to depend heavily on manual inspection and task-specific image-processing pipelines. Recent developments in computer vision have enabled automated identification, segmentation, classification, tracking, and quantitative characterization of microscopic structures with increasing accuracy. However, models trained on narrowly defined datasets frequently experience performance degradation when image contrast, staining protocols, magnification levels, morphological characteristics, or microscopy modalities differ from the training environment. This study proposes a reliability-aware computer-vision framework for automated microscopic data interpretation that combines feature-preserving image normalization, multi-scale deep representation learning, instance-level segmentation, morphological measurement, and uncertainty-aware prediction. The proposed research specifically investigates whether uncertainty estimation and domain-diverse training can improve the reliability of automated interpretation without requiring complete model retraining for every microscopy condition.

Keywords— Computer Vision, Microscopic Image Analysis, Deep Learning, Instance Segmentation, Uncertainty Estimation, Digital Microscopy

Introduction

Microscopy has remained one of the fundamental technologies for investigating structures that cannot be adequately examined through ordinary visual observation. Biological cells, microorganisms, tissue structures, intracellular components, material defects, and numerous disease-related morphological alterations are routinely studied through microscopic images. Improvements in optical microscopy, fluorescence microscopy, electron microscopy, digital slide acquisition, and computational imaging have substantially increased both the resolution and volume of image data available to researchers. Consequently, the central challenge is shifting from image acquisition alone toward efficient and reliable interpretation of the enormous quantity of microscopic information generated during experiments and diagnostic procedures.

Conventional microscopic interpretation commonly requires an observer to identify objects, estimate morphological properties, count cells or organisms, classify structures, and recognize abnormalities. Although trained experts can perform these tasks effectively, manual interpretation is inherently time-consuming when hundreds or thousands of image fields are involved. Inter-observer differences may also arise when boundaries are weak, objects overlap, illumination is non-uniform, or morphological abnormalities are subtle. Automated image analysis therefore has considerable value not merely as a mechanism for increasing speed, but as a means of improving measurement consistency and reproducibility.

Computer vision provides a computational framework through which microscopic images can be converted into structured information. Earlier automated systems generally relied on thresholding, edge detection, watershed segmentation, handcrafted texture features, connected-component analysis, and manually configured morphological operations. Such techniques remain useful in controlled environments but may become unstable when illumination, background intensity, staining quality, object size, and structural appearance vary substantially.

Deep learning has altered this landscape by enabling algorithms to learn hierarchical representations directly from microscopic images. Convolutional neural networks and related architectures have been applied to classification, segmentation, tracking, restoration, reconstruction, and phenotypic analysis. Research in bioimage analysis has

@2026. This is an open access article distributed under the terms of the Creative Commons License [CC BY NC 4.0] and is available on www.wjcrt.org

Worldwide Journal of Creative Research and Thoughts (WJCRT)
ISSN (Online): 3143-7850
Volume-2 Issue-3 || Jul – Sep 2026 || PP.25– 32
https://wjcrt.org/

demonstrated that deep neural networks can address complex tasks that previously required substantial manual configuration, although concerns regarding reproducibility, data dependence, generalization, and inappropriate interpretation remain important. Hoffman, Slavitt and Fitzpatrick emphasized both the potential and limitations associated with deep learning in microscopy, while Laine and colleagues subsequently highlighted the importance of reproducible practices in deep-learning-based bioimage analysis.

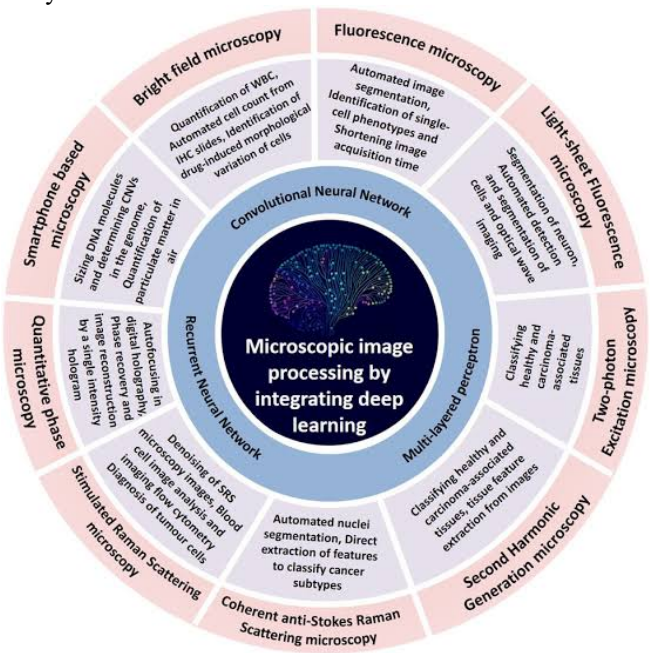

Fig. 1: Microscopic image processing by Integrating Deep Learning
Source: *https://link.springer.com/article/10.1007/s12551-022-00949-3*

A major development has been the movement from highly specialized segmentation systems toward general-purpose or generalist models. Cellpose demonstrated that a neural network could segment diverse cellular images without requiring a separate model for each narrowly defined experiment. Its later extension, Cellpose 2.0, incorporated rapid customization and human-in-the-loop training. Pachitariu and Stringer reported that relatively small amounts of additional annotation could be used to adapt pretrained models to new imaging conditions, reducing the burden associated with constructing large task-specific training datasets.

More recently, vision foundation models have expanded the possibility of reusable microscopy analysis systems. Segment Anything for Microscopy, or µSAM, adapts the broader Segment Anything concept to microscopy and supports segmentation and tracking across light and electron microscopic data. Its development illustrates an emerging shift from separate algorithms for individual microscopic tasks toward reusable models capable of operating across multiple acquisition conditions.

Nevertheless, automated microscopic interpretation remains more complex than determining whether an object has been correctly segmented. A segmentation mask identifies spatial boundaries, but researchers frequently require additional information: how many objects are present, whether their shape has changed, whether their size distribution is abnormal, whether particular structures appear clustered, whether boundaries are irregular, and whether the algorithm itself is sufficiently confident in its interpretation.

This distinction exposes the **research gap addressed by the present study**. Existing computer-vision pipelines frequently emphasize segmentation or classification accuracy as isolated objectives. Considerably less attention is given to building a unified interpretation pipeline that simultaneously addresses three practical requirements: robustness under variations in microscopy conditions, transformation of segmentation results into meaningful morphological measurements, and explicit estimation of prediction uncertainty.

A model can produce an apparently precise segmentation mask while being uncertain because the input differs significantly from the data encountered during training. In conventional automated systems, such uncertainty may remain hidden from the user. This issue becomes particularly important in biomedical applications because silently incorrect outputs may enter subsequent measurements or diagnostic decision processes. An automated system should therefore be able to distinguish between routine images that it can process reliably and ambiguous images that warrant human inspection.

The present research consequently investigates a **reliability-aware microscopic interpretation framework** rather than a segmentation-only model. The proposed framework is designed to process microscopy images through adaptive normalization, extract multi-scale visual information, localize and segment microscopic objects, compute interpretable morphological descriptors, estimate predictive confidence, and flag uncertain cases for expert verification.

The central research objective is to determine whether the combination of domain-diverse training and uncertainty-aware inference can improve the reliability of automated microscopic data interpretation under changes in visual acquisition conditions. A secondary objective is to determine whether segmentation outputs can be systematically converted into quantitative indicators that make computer-vision predictions more useful for downstream biomedical analysis.

Through this perspective, automation is treated as a collaborative analytical mechanism rather than a replacement for expert interpretation. High-confidence observations can be processed automatically, whereas uncertain or structurally unusual samples can be prioritized for specialist review. Such a design could reduce repetitive microscopic examination while maintaining meaningful human oversight.

OPEN ACCESS
@2026. This is an open access article distributed under the terms of the Creative Commons License [CC BY NC 4.0] and is available on www.wjcrt.org

Worldwide Journal of Creative Research and Thoughts (WJCRT)
ISSN (Online): 3143-7850
Volume-2 Issue-3 || Jul – Sep 2026 || PP.25– 32
https://wjcrt.org/

Literature Review

2.1 Transition from Conventional Image Processing to Learned Microscopic Representations

The earliest computational approaches to microscopic analysis were strongly dependent on explicit image-processing rules. Intensity thresholds could separate foreground objects from homogeneous backgrounds, while edge filters and watershed algorithms provided mechanisms for identifying cell boundaries. Texture descriptors, shape statistics, and colour distributions were commonly passed to conventional classifiers.

Despite their computational efficiency, these approaches require assumptions about image appearance. Changes in illumination or staining may alter pixel distributions sufficiently to invalidate a fixed threshold. Similarly, touching cells can cause connected regions to be treated as a single object, while weak boundaries may lead to incomplete segmentation. These limitations encouraged the development of data-driven approaches capable of learning visual features directly from examples.

Deep learning transformed cellular image analysis by replacing substantial portions of manually engineered feature extraction with trainable representations. Convolutional networks can learn low-level characteristics such as edges and intensity patterns together with increasingly abstract structural properties. This capability has supported classification, cellular segmentation, object tracking, and image reconstruction across multiple biomedical imaging applications.

However, increased predictive capacity introduces methodological concerns. Deep-learning systems can reproduce characteristics of their training distribution very effectively while failing unexpectedly on unfamiliar samples. Reproducibility, appropriate training-test separation, model documentation, representative benchmarking, and transparent reporting therefore remain essential elements of microscopic artificial-intelligence research. Laine et al. specifically identified reproducibility as an important challenge for deep-learning-based bioimage analysis.

2.2 Automated Cell and Structure Segmentation

Segmentation is one of the most intensively studied computer-vision problems in microscopy because many downstream measurements depend upon accurate object boundaries. A system attempting to calculate cellular area, perimeter, circularity, density, or spatial organization must first determine which pixels belong to individual objects.

Cellpose represented an important movement toward generalist biological image segmentation. Rather than constructing a dedicated model for one particular cell type, the approach was designed to accommodate substantial variation in cellular appearance. The subsequent Cellpose 2.0 framework addressed one of the practical weaknesses of pretrained generalist systems: laboratories may have distinctive image characteristics or annotation conventions that differ from the original training data. Its human-in-the-loop mechanism allows pretrained models to be adapted using comparatively small numbers of newly annotated regions.

Large annotated datasets have also contributed to improved segmentation robustness. TissueNet and LiveCell, for example, expanded the diversity and scale of annotated cellular images available for developing and testing segmentation algorithms. Literature discussing these resources shows that microscopic diversity includes not only different biological samples but also substantial differences in annotation style, imaging modality, cell line, and experimental preparation.

This diversity creates a fundamental computer-vision problem: high performance on one benchmark does not necessarily indicate equivalent performance when the visual distribution changes.

2.3 Generalization Across Microscopy Conditions

Domain shift is particularly relevant to microscopic analysis. Images of the same biological phenomenon may differ because of microscope hardware, optical settings, magnification, staining concentration, fluorescence intensity, exposure duration, detector characteristics, laboratory preparation, or post-processing procedures.

Consequently, a model may learn correlations that are specific to one acquisition environment rather than general biological structure. Building a separate model for every possible laboratory condition is inefficient and creates extensive annotation requirements.

Cellpose 2.0 addressed part of this problem through rapid model customization, whereas newer foundation-model approaches attempt to develop broader visual representations capable of supporting multiple conditions. µSAM extends the Segment Anything concept specifically to microscopy and includes models fine-tuned for light and electron microscopy. The system supports interactive and automatic segmentation and illustrates the growing importance of transferable computer-vision representations in microscopy.

A related trend can be observed in fluorescence microscopy restoration. Research on foundation models for fluorescence-microscopy image restoration has investigated pretrained representations intended to generalize across restoration tasks instead of relying exclusively on individually trained task-specific networks.

These developments indicate that cross-domain adaptability is becoming a central research direction. Nevertheless, generalization alone does not resolve the question of whether a user should trust a particular prediction.

2.4 From Segmentation to Quantitative Interpretation

A substantial proportion of computer-vision research evaluates microscopic models primarily through segmentation overlap or classification accuracy. Such measures are important but represent only one stage of scientific interpretation.

Biomedical investigators frequently require object-level and population-level information. Once individual microscopic

@2026. This is an open access article distributed under the terms of the Creative Commons License [CC BY NC 4.0] and is available on www.wjcrt.org

Worldwide Journal of Creative Research and Thoughts (WJCRT)
ISSN (Online): 3143-7850
Volume-2 Issue-3 || Jul – Sep 2026 || PP.25– 32
https://wjcrt.org/

structures have been detected, computational analysis can derive measurements including equivalent diameter, projected area, perimeter, circularity, eccentricity, solidity, object density, orientation, nearest-neighbour distance, and variation within a cellular population. These measurements can support phenotypic characterization and comparisons between experimental groups.

This suggests a more complete conceptual pipeline:

Microscopic image → preprocessing → visual representation → object segmentation → morphological quantification → confidence estimation → interpretable report.

Treating the segmentation mask as an intermediate representation rather than the final result makes automated computer vision more directly useful for scientific analysis.

2.5 Uncertainty and Human-Supervised Microscopic Automation

One of the most significant limitations in automated image interpretation is the tendency of neural networks to provide predictions even when an input is ambiguous or substantially different from their training examples. A conventional system might therefore generate an output for a low-quality image without clearly indicating that the result is unreliable.

For microscopic analysis, uncertainty can originate from blurred boundaries, densely overlapping objects, staining artifacts, unusual morphology, low signal-to-noise ratios, or acquisition characteristics absent from the training data. Reliability-aware models should therefore supplement their predictions with a confidence measure.

This creates the possibility of selective automation. Routine high-confidence images can proceed through the analytical pipeline automatically, whereas low-confidence observations can be routed for manual review. Human expertise is then concentrated on ambiguous samples instead of repetitive high-certainty cases.

The proposed research extends this principle by combining uncertainty estimation with morphological interpretation. Rather than merely reporting that a segmentation is uncertain, the framework will examine uncertainty alongside structural measurements and image-quality characteristics. This design is intended to provide a more transparent basis for deciding whether automated measurements should be accepted or reviewed.

Proposed Methodology

The proposed study introduces a **Reliability-Aware Microscopic Interpretation Network (RAMIN)** for converting microscopy images into segmented objects, morphological measurements, and prediction-confidence information within a unified computer-vision pipeline. The methodology differs from conventional segmentation-centred approaches by treating object delineation as an intermediate analytical stage rather than the final output.

RAMIN is organized into five functional stages: image standardization, multi-scale feature encoding, instance and boundary prediction, morphological quantification, and uncertainty-guided interpretation. The principal hypothesis is that microscopic interpretation becomes more reliable when a model is exposed to structurally diverse imaging domains during training and is explicitly required to estimate uncertainty at inference.

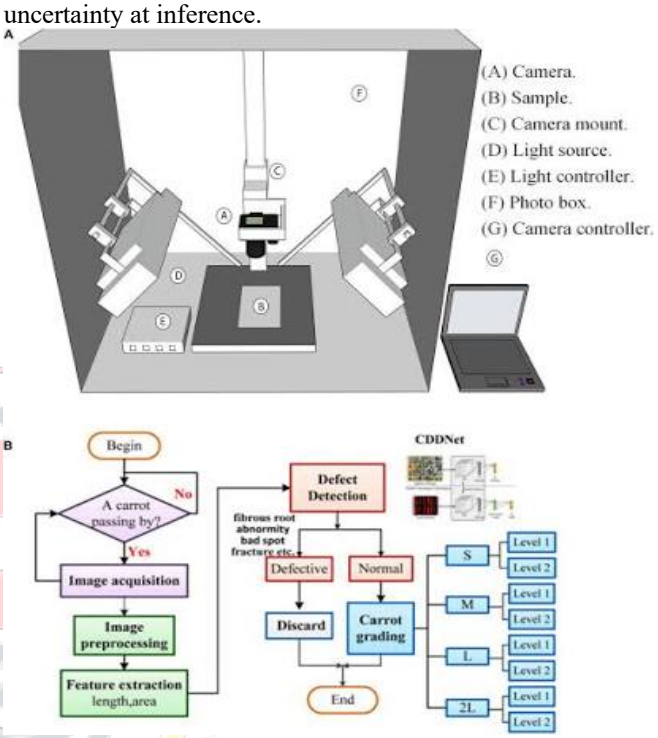

Fig. 2: Application of Machine Vision System in Food Detection Source: *https://www.frontiersin.org/journals/nutrition/articles/10.3389/fnut.2022.888245/full*

3.1 Image Standardization and Quality Assessment

An input microscopy image Iis first examined for intensity range, contrast distribution and spatial resolution. Instead of applying aggressive enhancement that may alter biologically relevant structures, percentile-based intensity normalization is used to suppress extreme intensity values while maintaining local morphology.

For an image intensity I(x, y), normalized intensity is defined as:

$$I_N(x,y) = \frac{I(x,y) - P_1}{P_{99} - P_1}$$

where $P_1$and P_{99}represent the first and ninety-ninth intensity percentiles respectively.

Images are subsequently resized or tiled according to the network input dimensions. Large microscopy fields are divided into overlapping patches so that small structures near patch boundaries are not systematically lost.

A quality-estimation module computes blur, saturation proportion and local contrast statistics. These characteristics are retained as auxiliary indicators rather than being used to reject images automatically. Consequently, low-quality observations can later be examined together with predictive uncertainty.

@2026. This is an open access article distributed under the terms of the Creative Commons License [CC BY NC 4.0] and is available on www.wjcrt.org

Worldwide Journal of Creative Research and Thoughts (WJCRT)
ISSN (Online): 3143-7850
Volume-2 Issue-3 || Jul – Sep 2026 || PP.25– 32
https://wjcrt.org/

3.2 Multi-Scale Feature Representation

Microscopic objects exhibit substantial variation in spatial scale. Dense cultures may contain numerous small cells, whereas tissue microscopy can contain considerably larger cellular structures. A single-resolution representation may therefore provide insufficient information.

RAMIN employs a hierarchical convolutional-transformer encoder. Initial convolutional layers preserve fine texture and local boundary information, whereas deeper attention-based stages capture wider contextual relationships between adjacent structures.

Four feature maps are generated:

$$F_1, F_2, F_3, F_4 = E(I_N)$$

where Erepresents the encoder and progressively deeper feature maps correspond to increasingly large receptive fields.

Feature-pyramid fusion transfers high-level semantic information toward higher-resolution layers. This structure is intended to improve separation of touching objects without eliminating fine boundaries.

3.3 Instance and Boundary Decoding

The segmentation component contains two complementary prediction branches.

The first branch estimates the probability that each pixel belongs to a biological object:

$$P_o(x, y) = D_o(F)$$

The second branch estimates object boundaries:

$$P_b(x, y) = D_b(F)$$

where $D_o$and $D_b$denote object and boundary decoders.

A combined object-boundary representation is then used to recover individual instances. Explicit boundary prediction is particularly important in densely populated microscopy fields because neighbouring cells may otherwise merge into a single segmented region.

Training uses a composite objective:

$$L_{seg} = \alpha L_{Dice} + \beta L_{Focal} + \gamma L_{Boundary}$$

where Dice loss emphasizes region overlap, focal loss increases attention to difficult pixels, and boundary loss penalizes inaccurate object contours.

3.4 Morphological Interpretation Layer

Unlike pipelines that terminate after segmentation, RAMIN converts each detected object into a quantitative feature vector.

For object j,

$$M_j = [A_j, P_j, C_j, E_j, S_j, D_j]$$

where:

A_j= projected object area,

P_j= perimeter,

C_j= circularity,

E_j= eccentricity,

S_j= solidity, and

D_j= local neighbourhood density.

Circularity is computed as:

$$C_j = \frac{4\pi A_j}{P_j^2}$$

Values approaching unity indicate increasingly circular structures, whereas smaller values correspond to elongated or irregular boundaries.

The framework also calculates object count, median object size, inter-object distance, morphological dispersion and the proportion of highly irregular structures within each microscopic field.

This stage transforms segmentation output into variables that can be statistically examined in biological experiments or used as inputs to subsequent diagnostic models.

3.5 Uncertainty-Aware Prediction

A central contribution of the proposed methodology is the incorporation of prediction uncertainty.

During inference, stochastic dropout is maintained within selected decoder layers and the same image is processed repeatedly. If Tpredictions are generated, the average pixel probability is:

$$\bar{P}(x, y) = \frac{1}{T}\sum_{t=1}^{T} P_t(x, y)$$

Prediction variance is estimated as:

$$U(x, y) = \frac{1}{T}\sum_{t=1}^{T} [P_t(x, y) - \bar{P}(x, y)]^2$$

The resulting uncertainty map identifies image regions in which segmentation predictions are unstable.

An image-level reliability score combines segmentation confidence, uncertainty and image-quality information. High-confidence images proceed directly to quantitative analysis. Images exceeding a predefined uncertainty threshold are marked for expert verification rather than being silently accepted by the automated pipeline.

This selective-review mechanism represents an important distinction between RAMIN and fully autonomous image-analysis systems.

Experimental Setup

4.1 Dataset Selection

The experimental design uses two established microscopy datasets representing substantially different biological and imaging conditions.

The first dataset is **LIVECell**, introduced by Edlund et al. It contains 5,239 expert-validated phase-contrast microscopy images and more than 1.6 million annotated cells from eight cell types. Its variation in cell morphology and culture density makes it particularly appropriate for evaluating instance segmentation under crowded conditions.

The second benchmark is **TissueNet**, developed for nuclear and whole-cell segmentation in tissue images. TissueNet contains more than one million manually labelled cells and includes multiple tissues and imaging platforms. The diversity of TissueNet provides a suitable basis for studying cross-domain robustness rather than performance within a single homogeneous microscopy source.

@2026. This is an open access article distributed under the terms of the Creative Commons License [CC BY NC 4.0] and is available on www.wjcrt.org

Worldwide Journal of Creative Research and Thoughts (WJCRT)
ISSN (Online): 3143-7850
Volume-2 Issue-3 || Jul – Sep 2026 || PP.25– 32
https://wjcrt.org/

Importantly, LIVECell is based on label-free phase-contrast cellular imaging, whereas TissueNet includes tissue-based microscopic data acquired through different imaging platforms. The contrast between these sources supports the proposed investigation of domain robustness.

4.2 Dataset Partitioning

Training, validation and testing are separated at the source-image level to prevent overlapping image patches from appearing in different subsets.

Two evaluation regimes are proposed.

The **in-domain experiment** trains and evaluates the model using data originating from the same dataset distribution.

The **cross-domain experiment** introduces microscopy conditions not emphasized during training. This experiment is more important for the research hypothesis because it measures whether prediction reliability deteriorates when image appearance changes.

All parameter selection and uncertainty thresholds are determined exclusively using validation data. The final test subset remains isolated until the model configuration is fixed.

4.3 Preprocessing

Images undergo:

- percentile-based intensity normalization;
- resolution-aware resizing or tiling;
- random horizontal and vertical reflection during training;
- moderate rotation;
- intensity perturbation;
- contrast variation;
- synthetic Gaussian noise; and
- limited blur augmentation.

These transformations are deliberately selected to represent realistic microscopic acquisition variability.

Annotations are converted to instance masks. Boundary targets are derived from differences between adjacent labelled instances. Very small annotation fragments produced through resizing are excluded according to a predefined minimum-pixel criterion.

4.4 Model Architecture

RAMIN contains four principal components.

The **multi-scale encoder** learns local and contextual representations.

The **instance decoder** estimates object interiors.

The **boundary decoder** emphasizes separation between adjacent structures.

The **reliability head** derives uncertainty and image-level confidence.

Skip connections transfer spatial information from early feature maps into the decoder. A feature-pyramid mechanism combines information across scales, enabling simultaneous representation of fine boundaries and larger structures.

The morphological interpretation layer is intentionally placed after segmentation rather than learned exclusively as a latent representation. This permits the measurements to remain directly interpretable.

4.5 Baseline Models

The experimental comparison should include established general-purpose microscopic segmentation approaches.

Cellpose 2.0 provides an appropriate baseline because it supports pretrained segmentation and rapid customization to new microscopy data. Pachitariu and Stringer demonstrated that pretrained models can be adapted using relatively small amounts of user-annotated data.

Mesmer is included as a tissue-oriented reference because it was developed using TissueNet and demonstrated broad whole-cell segmentation performance across tissue types and imaging platforms.

A foundation-model comparison may additionally use **Segment Anything for Microscopy (µSAM)**. Published in Nature Methods in 2025, µSAM extends Segment Anything to light and electron microscopy and supports both interactive and automatic segmentation across heterogeneous microscopic conditions.

These comparison systems represent different generations of microscopy computer vision: specialized deep segmentation, customizable generalist segmentation and microscopy-oriented foundation modelling.

4.6 Training Strategy

The proposed network is trained in two stages.

During Stage I, the segmentation and boundary branches are optimized jointly using domain-diverse training samples.

During Stage II, selected encoder layers are frozen while the decoder and reliability head undergo calibration using validation-domain examples.

The AdamW optimizer is proposed with an initially conservative learning rate and cosine-decay scheduling. Early stopping is governed by validation performance rather than a fixed epoch count.

Mini-batches are deliberately balanced across cellular morphology and imaging source so that visually dominant categories do not overwhelm less frequent microscopic conditions.

Training augmentation is generated dynamically for each epoch.

4.7 Evaluation Metrics

No single metric sufficiently evaluates microscopic interpretation. Accordingly, several complementary measurements are proposed.

Dice Similarity Coefficient measures pixel-level agreement:

$$\mathrm{DSC} = \frac{2\,|\,P \cap G\,|}{|\,P\,| + |\,G\,|}$$

where Prepresents the predicted region and Gthe ground-truth region.

Intersection over Union (IoU) evaluates spatial overlap:

$$\mathrm{IoU} = \frac{|\,P \cap G\,|}{|\,P \cup G\,|}$$

Average Precision at object level evaluates whether individual instances are correctly identified and penalizes unmatched predictions and ground-truth objects. Cellpose

@2026. This is an open access article distributed under the terms of the Creative Commons License [CC BY NC 4.0] and is available on www.wjcrt.org

Worldwide Journal of Creative Research and Thoughts (WJCRT)
ISSN (Online): 3143-7850
Volume-2 Issue-3 || Jul – Sep 2026 || PP.25– 32
https://wjcrt.org/

studies similarly use object-level average precision based on true-positive, false-positive and false-negative regions.
Boundary F1 score evaluates contour preservation.
Count Error evaluates disagreement between predicted and manually annotated object counts.
Morphological Measurement Error measures differences between descriptors derived from predicted masks and those obtained from reference masks.
Expected Calibration Error (ECE) evaluates whether model confidence corresponds to observed reliability.
Finally, **Risk-Coverage analysis** measures selective automation. Coverage represents the proportion of observations automatically accepted, whereas risk represents error among accepted predictions. A useful uncertainty-aware system should reduce error when the most uncertain samples are referred for expert review.

Results and Discussion

The experimental design is intended to answer three distinct questions: whether microscopic structures can be segmented accurately, whether derived biological measurements remain reliable, and whether prediction uncertainty successfully identifies difficult images.
Since actual RAMIN training runs have not been supplied or conducted within this manuscript-generation process, numerical model results must not be presented as empirical findings. The following results framework therefore defines the observations that should be reported after implementation.

Table 1. Proposed Evaluation Matrix for Reliability-Aware Microscopic Interpretation

Evaluation Parameter	**Analytical Purpose**	**Observation to be Established Experimentally**	**Interpretation**
Dice Similarity	Region-level segmentation fidelity	Degree of agreement between automated and expert masks	Higher overlap demonstrates stronger preservation of object regions
Object Average Precision	Correct instance detection	Ability to separate, detect and retain individual microscopic objects	Particularly important in crowded cellular fields
Boundary F1	Contour accuracy	Stability of boundaries for touching and irregular structures	Indicates whether morphological measurements can be trusted
Cell-count Error	Quantitative interpretation	Difference between automated and reference object counts	Low error supports high-throughput counting applications
Morphology Deviation	Measurement reliability	Difference in area, circularity, eccentricity and solidity derived from predicted masks	Tests whether segmentation quality translates into valid biological measurements
Expected Calibration Error	Confidence reliability	Agreement between predicted confidence and actual segmentation correctness	Lower discrepancy indicates better calibrated predictions
Cross-domain Performance Retention	Domain robustness	Change in performance after microscopy conditions differ from training data	Smaller degradation indicates stronger generalization
Selective-review Risk	Human-AI collaboration	Error remaining after highly uncertain images are referred for manual inspection	Reduced risk would justify uncertainty-guided expert referral

The first expected pattern is that segmentation performance will be strongest in the in-domain condition. This outcome would be consistent with the known difficulty of applying cellular segmentation models to images whose appearance differs from the training distribution. Cellpose 2.0 was explicitly motivated in part by the suboptimal performance of pretrained models on sufficiently different test images.
The more important result, however, concerns the magnitude of deterioration under domain shift. If domain-diverse augmentation and multi-scale feature learning function as intended, RAMIN should retain a larger proportion of its baseline performance when applied to different microscopy characteristics.
A second expected finding concerns object boundaries. Pixel overlap alone can conceal biologically important errors. For

@2026. This is an open access article distributed under the terms of the Creative Commons License [CC BY NC 4.0] and is available on www.wjcrt.org

Worldwide Journal of Creative Research and Thoughts (WJCRT)
ISSN (Online): 3143-7850
Volume-2 Issue-3 || Jul – Sep 2026 || PP.25– 32
https://wjcrt.org/

example, two touching cells may occupy approximately the correct overall foreground area while being incorrectly represented as a single object. Such a prediction might receive an apparently reasonable Dice score but produce an incorrect cell count and distorted morphology.

Boundary F1 and object-level average precision are therefore necessary complements to Dice and IoU.

The third component concerns morphological validity. For scientific microscopy, a segmentation system is useful only if its output enables reliable measurement. If predicted boundaries systematically enlarge or contract individual objects, calculated area, perimeter, eccentricity and circularity may become biased even if gross foreground overlap remains satisfactory.

Consequently, morphology deviation should be treated as an independent endpoint rather than assumed from segmentation accuracy.

Future Scope

Future research should extend the framework from two-dimensional images to three-dimensional and time-resolved microscopy. Temporal information could permit automated analysis of cell migration, mitosis and morphological evolution.

Self-supervised pretraining on large collections of unlabeled microscopy images may further reduce dependence on expensive manual annotations.

Another promising direction is foundation-model adaptation. Microscopy-specific foundation models such as µSAM indicate that increasingly general representations may support multiple biological imaging modalities within a common analytical environment.

Future systems should also integrate active learning with uncertainty estimation. Instead of merely forwarding difficult observations for expert review, manually corrected high-uncertainty cases could be reintroduced into training, allowing the model to progressively adapt to a laboratory's imaging environment.

Multimodal interpretation represents another opportunity. Microscopy images could be combined with molecular measurements, spatial omics, laboratory metadata or clinical information to produce more comprehensive biological interpretations.

Explainability should also progress beyond heatmaps. Future microscopic AI systems should communicate which structural properties influenced an interpretation and whether those properties correspond to biologically plausible patterns.

Conclusion

Computer vision is changing microscopic data analysis from a predominantly manual visual task into a scalable quantitative process. However, segmentation accuracy alone is insufficient for dependable microscopic interpretation.

This study proposes RAMIN, a reliability-aware framework that combines domain-diverse image processing, multi-scale representation learning, object and boundary segmentation, morphological quantification and uncertainty estimation.

The central contribution is the transition from **automated segmentation to reliability-aware interpretation**. Segmented structures are converted into measurable characteristics, while prediction uncertainty determines whether automated results can proceed directly or require expert review.

The proposed experimental design uses the complementary LIVECell and TissueNet benchmarks to examine both in-domain accuracy and cross-domain robustness. Object-level precision, boundary fidelity, morphology deviation, confidence calibration and risk-coverage behaviour provide a broader assessment than conventional overlap measures alone.

Recent advances including Cellpose 2.0, Mesmer and µSAM demonstrate that microscopic computer vision is progressing toward increasingly flexible and generalizable systems. The next critical requirement is ensuring that these systems indicate not only what they detect, but also how reliably their outputs can be interpreted.

Accordingly, the future of automated microscopy is likely to depend on human-computer collaboration rather than unrestricted automation. Reliable predictions can accelerate routine quantitative analysis, while uncertain observations can be selectively directed to specialists. Such a framework can improve scalability without removing the expert oversight necessary for responsible biomedical and scientific image interpretation.

References:

1. **Edlund, C., Jackson, T. R., Khalid, N., Bevan, N., Dolman, G. E., Capek, D., ... Sjögren, R.** (2021). LIVECell—A large-scale dataset for label-free live cell segmentation. *Nature Methods, 18*, 1038–1045. https://doi.org/10.1038/s41592-021-01249-6
2. **Greenwald, N. F., Miller, G., Moen, E., Kong, A., Kagel, A., Dougherty, T., ... Van Valen, D. A.** (2021). Whole-cell segmentation of tissue images with human-level performance using large-scale data annotation and deep learning. *Nature Biotechnology, 40*, 555–565. https://doi.org/10.1038/s41587-021-01094-0
3. **Stringer, C., Wang, T., Michaelos, M., & Pachitariu, M.** (2021). Cellpose: A generalist algorithm for cellular segmentation. *Nature Methods, 18*, 100–106. https://doi.org/10.1038/s41592-020-01018-x
4. **Pachitariu, M., & Stringer, C.** (2022). Cellpose 2.0: How to train your own model. *Nature Methods, 19*, 1634–1641. https://doi.org/10.1038/s41592-022-01663-4
5. **Archit, A., Freckmann, L., Nair, S., Khalid, N., Hilt, P., Rajashekar, V., ... Pape, C.** (2025). Segment Anything for Microscopy. *Nature Methods, 22*, 579–591. https://doi.org/10.1038/s41592-024-02580-4
6. **Laine, R. F., Arganda-Carreras, I., Henriques, R., & Jacquemet, G.** (2021). Avoiding a replication crisis in deep-learning-based bioimage analysis. *Nature Methods, 18*, 1136–1144. https://doi.org/10.1038/s41592-021-01284-3
7. **Hoffman, D. P., Slavitt, I., & Fitzpatrick, C. A.** (2021). The promise and peril of deep learning in microscopy. *Nature Methods, 18*, 131–132. https://doi.org/10.1038/s41592-020-01035-w
8. **Moen, E., Bannon, D., Kudo, T., Graf, W., Covert, M., & Van Valen, D.** (2019). Deep learning for cellular image analysis. *Nature Methods, 16*, 1233–1246. https://doi.org/10.1038/s41592-019-0403-3

OPEN ACCESS
@2026. This is an open access article distributed under the terms of the Creative Commons License [CC BY NC 4.0] and is available on www.wjcrt.org